2006

Air Source Heat Pump for Northern Climates Part II: Measurement and Verification

Stefan S. Bertsch
Purdue University

Eckhard A. Groll
Purdue University

David B. Bouffard
Purdue University

William J. Hutzel
Purdue University

AIR SOURCE HEAT PUMP FOR NORTHERN CLIMATES PART II: MEASUREMENT AND VERIFICATION

Stefan S. BERTSCH[1]*, Eckhard A. GROLL[2]*, David B. BOUFFARD[3], William J. HUTZEL[3]

*Purdue University
School of Mechanical Engineering
Ray W. Herrick Laboratories
West Lafayette, Indiana 47907, USA

[1]Corresponding Author, Tel: (765 496 2886), Fax: (765 494 0787), E-mail: sbertsch@purdue.edu
[2]Tel: (765 496 2201), Fax: (765 494 0787), E-mail: groll@purdue.edu

[3]Purdue University
Department of Mechanical Engineering Technology
West Lafayette, Indiana 47907, USA

ABSTRACT

Air source heat pumps are widely used for residential heating because of their relatively low installation costs. Major disadvantages are that the heat output and COP decrease and the discharge temperature of the compressor increases as the outdoor temperature decreases. All of these factors usually lead to the need of combined heat pump and backup heating systems, which increases the cost and lowers the efficiency of the overall system.

In this study, a novel air-source, two-stage heat pump using R-410A as the refrigerant was simulated, designed, constructed and tested for ambient temperatures as low as -30°C and supply temperatures of up to 50°C. In addition to air and water heating, the system is also able to provide sufficient air conditioning in cooling mode.

The study is divided into two parts. The first part entitled "Simulation of Different Heat Pump Cycles" summarizes the results of an extended literature and patent review, and presents a theoretical analysis of the three most promising cycles. The second part is entitled "Measurement and Verification" and focuses on the design, implementation, and testing of a breadboard system as well as on the comparisons with commercially available heat pumps.

1. INTRODUCTION

Based on the results of the analysis of several different refrigeration cycles (*Bertsch and Groll, 2005*), three heat pump cycles were chose for further investigations. Part I of this two-part paper (*Bertsch and Groll, 2006*) presented the simulation results of the economizer, intercooler and cascade cycles. A comparison of the three cycles was done on the basis of efficiency and heating capacity. In order to build a bread board system, several other criteria were taken into consideration. Table 1 lists some of these criteria with a coarse classification for the three systems.

The system utilizing an intercooler has excellent part load capabilities and therefore, also works well in air conditioning mode and defrost mode. Since it only uses one kind of refrigerant and standard components, the maintenance costs should be low. Oil management will be problematic as well as high heat supply temperatures, which lead to a very small intercooling effect and therefore, high discharge temperatures of the system.

The economizer cycle shares the same advantages but is easier to control and does not rely on the supply temperature to control the suction temperature of the high pressure-stage compressor. Therefore, the discharge temperatures can be kept at a lower level than for the intercooler cycle. Oil management is probably the most critical issue of this system.

The cascade cycle outperforms the other two systems at very low ambient temperatures, but is very difficult to adapt to air conditioning mode and heating mode in low load situations. The installation costs as well as the maintenance costs are considerably higher than for the other two systems because of the usage of two different refrigerants.

Table 1: Comparison of the advantages and disadvantages of the three investigated heat pump cycles

Criteria	Intercooler	Economizer	Cascade
COP	o	+	+
Part load capability	+	+	-
Discharge temperature	-	+	+
Control of the system	o	+	+
High supply temperatures	-	o	+
Air conditioning	+	+	o
Defrosting	+	+	o
Oil Management	-	-	+
Installation costs	o	o	-
Maintenance costs	+	+	-

+… positive, o… average, -…negative

Considering all of these factors, the economizer cycle combines good performance with reasonable effort and costs. Therefore, this concept was chosen to be experimentally investigated by building a bread board system and testing it in psychrometric chambers.

2. SETUP OF THE BREAD BORAD SYSTEM

Figure 1 shows a simplified schematic of the bread board system and Table 2 provides some details of the system components. The measurement instrumentation will be explained in the Section 3.

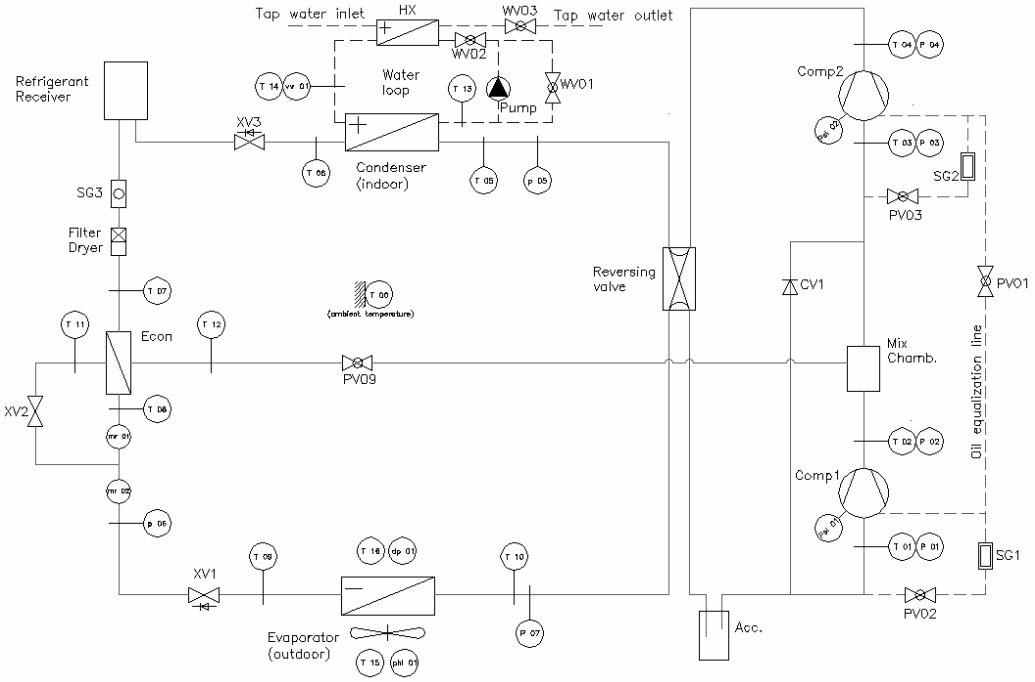

Figure 1: Simplified schematic and instrumentation of the two-stage heat pump system with economizing

On the right hand side, Compressor 1 (low pressure stage) and Compressor 2 (high pressure stage) can be seen with a mixing chamber in between. This mixing chamber ensures a good mixing of the injected two phase refrigerant with the hot discharge gas of the low pressure-stage compressor. A reversing valve enables the system to defrost and the check valve CV1 makes it possible to run Compressor 2 alone in single-stage heating mode. In heating mode the discharged refrigerant is directed to the indoor condenser, which is water cooled. For the test setup, a closed water loop was constructed in order to easily change the water flow-rate and inlet temperature for the condenser independently of each other. After leaving the condenser, the refrigerant bypasses the defrosting

expansion valve XV3 and flows over a sight glass and a filter/dryer into the economizer, where it is cooled by the injected refrigerant. At the outlet of the economizer the refrigerant is split into two parts. One part of the refrigerant (up to 30%) is expanded across expansion valve XV2 to the intermediate pressure. After exchanging heat in the economizer, it is injected into the mixing chamber to control the suction temperature of Compressor 2. The majority of the refrigerant is expanded across expansion valve XV1 instead of XV2 and then evaporates in the outdoor heat exchanger. The refrigerant returns to the compressor through the reversing valve and a suction line accumulator in order to protect the compressor from liquid refrigerant. This protection is especially important at startup and after a change in operating mode.

Table 2: List of the most important components of the schematic in Figure 1

#	Name	Description
1	Comp 1	Low pressure stage compressor, Scroll, 5.7 in^3/rev
2	Comp 2	High pressure stage compressor, Scroll, 3.0 in^3/rev
3	Reversing Valve	Standard reversing valve for R410A (5 ton)
4	Condenser	Flat plate heat exchanger – refrigerant to water (5 ton)
5	Evaporator	Custom made heat exchanger, 2m x 0.75m front area, 3 rows, 10 fins/inch
6	Econ.	Flat plate heat exchanger – refrigerant to refrigerant (1.5 ton)
7	Mix Chamb.	Coiled tube with refrigerant injector at the inlet
8	XV1	Expansion valve for the Evaporator with internal bypass, (5 ton)
9	XV2	Expansion valve for the Economizer (1.5 ton)
10	XV3	Expansion valve for defrosting mode (5 ton)
11	SG1, SG2	Sight glass to monitor the oil level inside the compressor
12	PV01	Plug valve to open and close the oil equalization line
13	PV09	Plug valve to close the injection line in single stage mode operation

The design was carried out for an estimated heating capacity of 17 kW (5 ton) at an ambient temperature of -10°C and a supply temperature of 50°C. Figure 2 shows the design of the system, created in a three-dimensional graphic program in order to achieve a good placement of all components. The larger compressor on the right hand side of the cart is the low pressure-stage compressor and the compressor on the left hand side the high pressure-stage compressor. The coiled tube in between is used as a mixing chamber. On the left back side, two mass flow meters can be seen. The economizer is the heat exchanger in middle of the back. The rest of the components on top of the cart are the reversing valve, filter, suction line accumulator, and several valves. On the lower level of the cart the water loop can be seen with the pump on the right hand side, the two heat exchangers, an expansion vessel, and several valves.

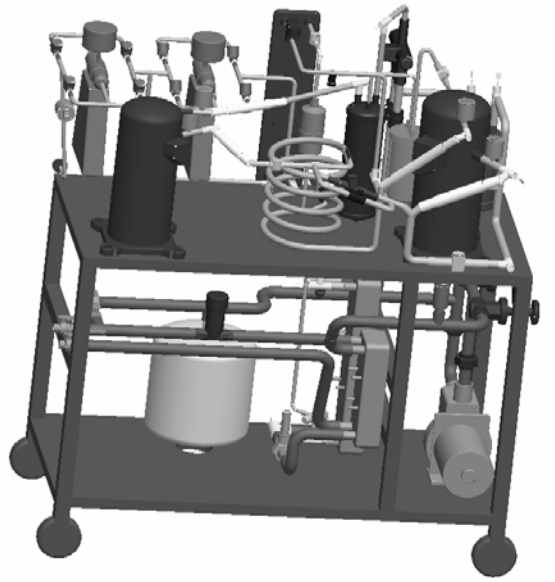

Figure 2: 3D - Design of the two stage heat pump cycle

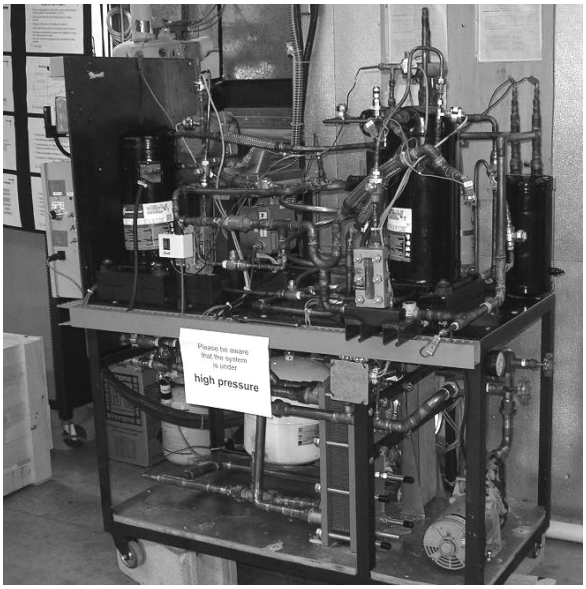

Figure 3: Picture of the main unit of the two stage heat pump cycle

Figure 3 shows the same arrangement as Figure 2, but in form of a picture of the actual bread board system. In addition to the components mentioned, the measurement equipment was added as well as sight glasses to measure the oil level in the compressors. The controls are located on the switchboard at the far left of the assembly.

Figure 4 shows a picture of the outdoor heat exchanger assembly which was especially designed for this project since no commercially available heat exchanger could be found for the given requirements. In particular, the frosting and defrosting behavior of the heat exchanger were optimized in order to assure optimum performance at very low ambient temperatures. The design worked very well and only little frost accumulation could be found during all testing due to the relatively small temperature difference between the refrigerant and ambient air of 3-6°C. The face area of the coil is approximately 1.5 m^2 and the shape of the coil is flat since no compressor needs to be enclosed in the outdoor unit. In order to improve drainage of the condensate the heat exchanger is installed in a slightly tilted position and the air is drawn through the coil by two fans with a fan diameter of 24 inches (610 mm). The combined approximate air flow rate is 10'000 m^3/h at a pressure drop of 35 Pa when running at full speed and 6'000 m^3/h at a pressure drop of 20 Pa in part load.

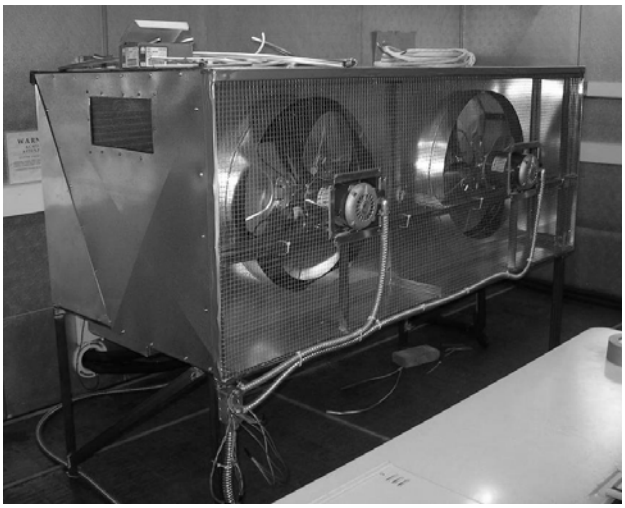

Figure 4: Picture of the outdoor heat exchanger with the angled coil located at the back and the two fans in front

3. MEASUREMENT INSTRUMENTATION AND DATA ANALYSIS

The performance of the system was measured at various outdoor temperatures and for two water supply temperatures of 40°C and 50°C. The outdoor temperatures in two-stage mode ranged from -28°C to -2°C and in single-stage mode from -15°C to 8°C. Data were collected after reaching steady state operation for about 25 minutes runtime with data collection every 10 seconds. The measurements were set up with a high level of redundancy in order to assure high accuracy.

3.1 Instrumentation

Over 40 T-type thermocouples were used to measure temperatures. Most transducers on the refrigerant side were immersed into the tube. For measurements on the air side, a grid of thermocouples was used. Eleven pressure and differential pressure transducers were located at various locations. The mass-flow rate of the refrigerant was measured before and after the injection with two Coriolis type mass flow-meters and the volume flow rate of water was determined using a turbine volume flow meter. A dew point meter with high accuracy was used to measure the humidity.

3.2 Determination of the oil level of the compressors

In order to measure the oil level inside the compressors, a bottom tap was drilled and an oil sight glass was mounted parallel to the compressor as shown in Figure 5. The top of the sight glass was connected through a plug valve to the suction line of the compressor. This assembly allows the determination of the oil level of the compressor during

downtime. When running the setup, the oil levels of both compressors were equalized at the beginning and then recorded after certain run times and equalized again.

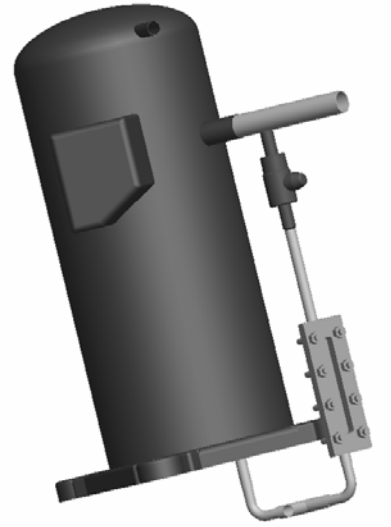

Figure 5: Schematic of the compressor with the sight glass for the determination of the oil level

3.3 Data Processing

The data reduction was carried out using the Engineering Equation Solver EES software (*Klein 2004*), which includes the fluid property information of the necessary refrigerants and fluids. The heating capacity of the heat pump was calculated using the temperature difference of the water across the heat exchanger together with the mass flow rate of the water as shown in Equation 1:

$$\dot{Q}_{H,W} = \dot{m}_w * C_p * \left(T_{w,o} - T_{w,i}\right) \tag{1}$$

Similarly the capacity of the outdoor unit was calculated using an energy balance knowing the inlet and outlet air temperatures and humidity and the air volume flow rate:

$$\dot{Q}_{C,A} = \dot{v}_A * \rho_A * \left(h_{A,o} - h_{A,i}\right) \tag{2}$$

Together with the measured electrical power consumption of the system, the coefficient of performance can be calculated:

$$COP_H = \frac{\dot{Q}_H}{P_{el,comp} + P_{el,aux}} \tag{3}$$

In order to determine the auxiliary electrical power consumption three approaches were used. One was to neglect auxiliary power in order to see the system performance, the second approach was to measure the power input of the outdoor fans and use the power consumption of a standard water pump as well as an estimate for the power consumption of the rest of the electric equipment. The third method was to use the formula given by ARI Standard 210/240 (*ARI 2003*):

$$P_{el,aux} = \left(\dot{Q}_H - P_{el,comp}\right) * 0.0341 \frac{kW}{kW} \tag{4}$$

In addition, an error analysis was conducted and the standard error propagation for all performance parameters was calculated according to:

$$\Delta x_{std} = \sqrt{\left(\frac{\partial x}{\partial u} \cdot \Delta u\right)^2 + \left(\frac{\partial x}{\partial v} \cdot \Delta v\right)^2} \tag{5}$$

The calculated error of the COP was between 3% and 9%, whereas the error of the capacity calculations was between 3% and 6%.

4. RESUTLS AND COMPARISON

The system worked very well from the beginning with only some minor changes and adjustments. In Figures 6 to 10 only the results of the final measurements are shown for a water supply temperature of 40°C. In most of these figures, three different operating modes are shown. The first one is two-stage mode with both compressors operating at 100% of their capacity. The second mode one is the high pressure-stage compressor operating alone with 100% capacity and the third mode one is the high pressure-stage compressor operating alone with 66% capacity in order to reduce the heating capacity at higher ambient temperatures.

Figure 6 shows the Coefficient of Performance in single-stage mode and two-stage mode versus the ambient temperature. At -15°C, the supply temperature had to be lowered to 37°C in order to not overheat the compressor. The main problem of the setup in this case is the high superheat at the inlet of the compressor due to the very long refrigeration piping with relatively little insulation. The efficiency of the single-stage mode with full compressor capacity is the highest since the heat exchangers are designed for the higher two-stage capacity. The decrease in compressor performance at a reduced speed of 40 Hz instead of 60 Hz is the dominating factor in the given application. The two-stage performance at high ambient temperatures is as expected lower than the performance in single-stage mode.

Figure 7 shows a comparison of the different COP calculations. The COP considering the actual measured auxiliary power consumption compares very well to the ARI Standard 210/240 (*ARI 2003*) calculation. The system COP without considering auxiliary power is as expected about 10% higher.

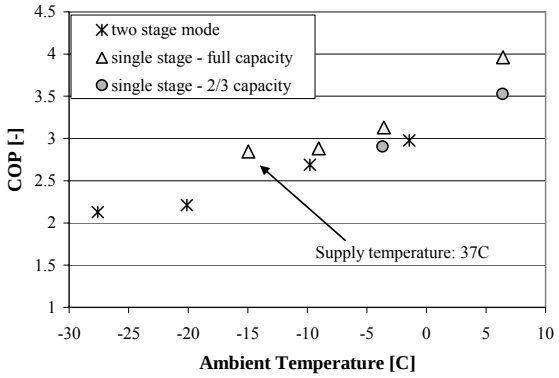

Figure 6: Coefficient of Performance not considering any auxiliary power consumption

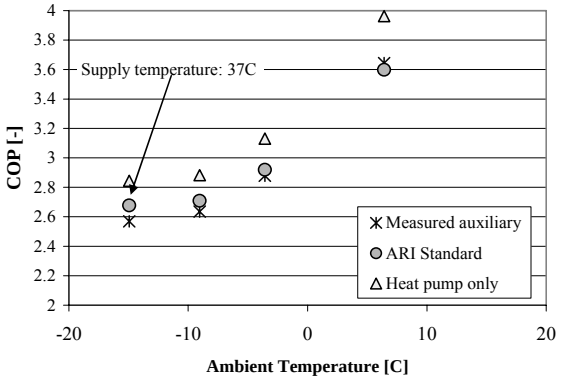

Figure 7: Coefficient of Performance considering the auxiliary power according to ARI guidelines and according to the measured values

Figure 8 shows the measured heating capacity during the three operating modes. As can be seen in Figure 8, the required capacity of 17kW at -10°C ambient temperature can be met almost exactly. Over the broad operating range from -15°C to 5°C ambient temperatures, the capacity of the system can be adjusted to the given load by switching in between the operating modes.

In order to calculate the second law efficiency, the COP calculated with the definition of the electrical power consumption according to the ARI standard 210/240 (*ARI 2003*) was used. The second law efficiency as shown in Figure 9 ranges from 38% to 46%. As already mentioned before, the part load efficiency is lower due to relatively low compressor efficiency in part load operation. The second law efficiency in single-stage mode is almost constant at 43% and the two-stage mode performance shows its best performance towards low ambient temperatures. The second law efficiency not considering the auxiliary electrical power consumption would exceed 50% at lower temperatures.

Figure 10 presents the discharge temperature of the high pressure-stage compressor as a function of outdoor temperature. In single-stage mode, it increases rapidly with decreasing ambient temperature, which leads to a limitation of the operating range. In two-stage mode, the discharge temperature can be kept below 105°C by regulating the superheat at the high pressure-stage compressor inlet to about 5°C.

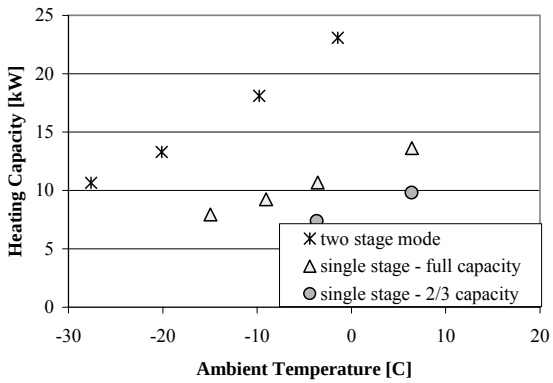

Figure 8: Heating capacity in different operating modes

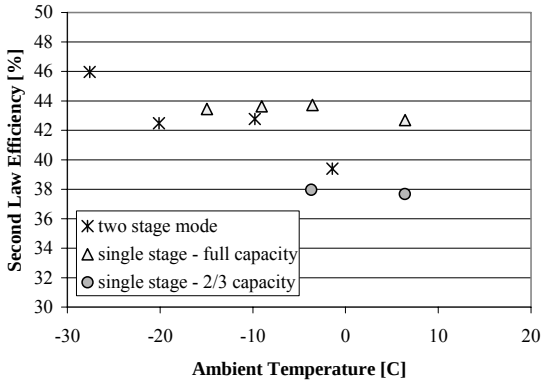

Figure 9: Second law efficiency in different operating modes

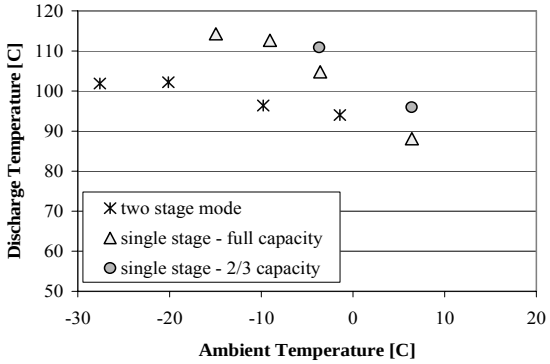

Figure 10: Discharge temperature of the high stage compressor in different operating modes

The experimental results obtained with the bread board system were compared to the simulation results presented in the part I paper and to the performance of a commercial heat pump (*Stein et al. 2005*). Figure 11 and 12 present the COP and heating capacity, respectively, as a function of outdoor temperature. As can be seen in Figure 11, the measured performance in single-stage mode matches the simulation results very well. In two-stage mode, the simulation results are approximately 20% higher than the achieved measurements, which is a good agreement considering the relatively simple model used for the simulations and the lack of compressor performance maps for the given operating range. The performance of the bread board system is as expected approximately 10% higher than the performance of a conventional system mainly due to the larger heat exchangers.

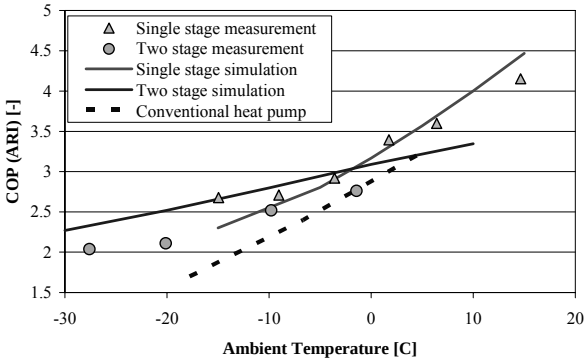

Figure 11: COP considering auxiliary power for the measurement, simulation and a conventional heat pump

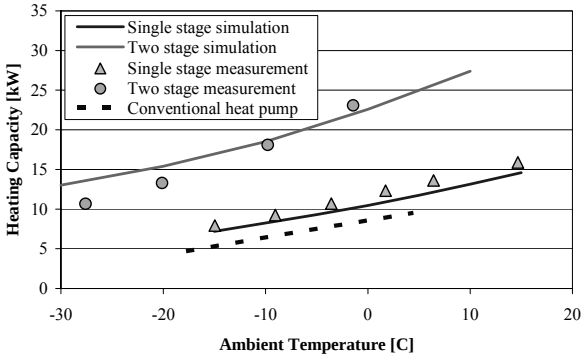

Figure 12: Heating capacity for the measurement, simulation and a conventional heat pump

Figure 12 indicates that the estimated heating capacity matches the simulation results very well for single-stage and two-stage operation and follows the trend of conventional heat pumps. Switching in between single stage and two stage mode means the capacity of the system can be more than doubled, which is a big advantage with respect to cycling of the heat pump.

Altogether the results for the bread board system exceeded the expectations and the chosen approach works very well. One of the challenges in the future will be to switch from a hand operated bread board system to a fully functional automated prototype system without the need of manual adjustments. A further issue is to replace the prototype components with commercially available components. Especially the low pressure-stage compressor with its single phase motor, displacement of 5.7 in^3/rev, and oil tap, and the reversible refrigerant receiver to store excess refrigerant at low operating temperatures are challenging.

5. CONCLUSIONS

A two-stage air to water heat pump was simulated, designed, built and tested. The functionality and concept of the system could be verified by showing that the heat pump is able to operate at ambient temperatures between -30°C and 10°C with supply water temperatures of up to 50°C. Discharge temperatures of the compressors in two-stage mode stayed below 105°C. Altogether the system shows a very high second law efficiency of approximately 40% to almost 50% over the whole operating range and outperforms most commonly used heat pump systems. The costs of the system are considerably higher than that of a common air source heat pump due to the need of a second compressor, an additional heat exchanger and a more complex control system.

The main challenges in the implementation of the system are an appropriate logic to control the system and to find commercially available compressors for the given specification. Especially the low pressure-stage compressor with an oil tap on the bottom or on the side of the compressor and a suction volume of 5.7in^3/rev are not commercially available for a single-phase R-410A compressor at the moment.

6. NOMENCLATURE

Symbol	Description	Unit	Index	Description
c_p	specific heat	[kJ/kg-K]	aux	Auxiliary
COP	Coefficient of Performance	[-]	C	Cooling
h	Enthalpy	[kJ/kg]	comp	Compressor
$\dot{m}$	Mass-flow-rate	[kg/s]	el	electric
ρ	Density	[kg/m^3]	H	Heating
T	Temperature	[°C]	I	Inlet
$\dot{Q}$	Heat rate	[kW]	O	Outlet
$\dot{v}$	Volume-flow-rate	[m^3/s]	R	Refrigerant
			W	Water

REFERENCES

ARI Standard 210/240 *Unitary Air-Conditioning and Air-Source Heat Pump Equipment*, 2003.

ASHRAE Standard 116, ANSI/ASHRAE 116-1995, *Methods of Testing for Rating Seasonal Efficiency of Unitary Air Conditioner and Heat Pumps*, American Society of Heating, Refrigeration and Air-conditioning Engineers, Inc., July 1995.

Bertsch S., Groll E.A., *Air to Water Heat Pump for Low Temperature Climates*, 8th International Energy Agency Heat Pump Conference, Las Vegas, NV, 2005

Bertsch S., Groll E.A., *Air Source Heat Pump for Northern Climates, Part I: Simulation of different heat pump cycles*, 11th International Refrigeration and Air Conditioning Conference at Purdue, 2006

Klein S.A., *EES, Engineering Equation Solver*, V7.173-3D, F_Chart Software, 1992-2004.

Stein J., Reid M., Krepchin I., and Santo Y., *Will the Low-Temperature Heat Pump Flatten Peak Heating Loads?*, Prospectus, E source Magazine, available at: www.esource.com, August 2005.

ACKNOWLEDGEMENT

This project was funded by Electro Industries, Inc. from Monticello, MN. The authors would like to acknowledge the support and initiative of Electro Industries, Inc. and William J. Seefeldt in particular.